Received: 16 November 2023 | Accepted: 18 March 2024

DOI: 10.1002/jev2.12429

RESEARCH ARTICLE

Synthetic biology-based bacterial extracellular vesicles displaying BMP-2 and CXCR4 to ameliorate osteoporosis

Han Liu[1,2,3,4] | **Peiran Song**[2,3,4] | **Hao Zhang**[1,2,3,4] | **Fengjin Zhou**[5] | **Ning Ji**[2,3,4] | **Mingkai Wang**[2,3,4] | **Guangyin Zhou**[2,3,4] | **Ruina Han**[2,3,4] | **Xinru Liu**[2,3,4] | **Weizong Weng**[2,3,4] | **Haoqi Tan**[2,3,4,6] | **Sicheng Wang**[2,3,4,7] | **Lei Zheng**[8] | **Yingying Jing**[2,3,4,9] | **Jiacan Su**[1,2,3,4]

[1]Department of Orthopedics, Xinhua Hospital, Shanghai Jiao Tong University School of Medicine, Shanghai, China

[2]Institute of Translational Medicine, Shanghai University, Shanghai, China

[3]Organoid Research Center, Shanghai University, Shanghai, China

[4]National Center for Translational Medicine (Shanghai) SHU Branch, Shanghai University, Shanghai, China

[5]Department of Orthopaedics, Honghui Hospital, Xi'an Jiao Tong University, Xi'an, China

[6]Suzhou Innovation Center of Shanghai University, Shanghai University, Suzhou, Jiangsu, China

[7]Department of Orthopedics, Shanghai Zhongye Hospital, Shanghai, China

[8]Department of Laboratory Medicine, Nanfang Hospital, Southern Medical University, Guangzhou, China

[9]Shaoxing Institute of Technology at Shanghai University, Shaoxing, China

Correspondence
Sicheng Wang, Department of Orthopedics, Shanghai Zhongye Hospital, Shanghai, China. Email: w.s.c@sina.com
Lei Zheng, Department of Laboratory Medicine, Nanfang Hospital, Southern Medical University, Guangzhou, China. Emial: nfyyzhenglei@smu.edu.cn

Yingying Jing, Institute of Translational Medicine, Shanghai University, Shanghai, China. Email: jingy4172@shu.edu.cn

Jiacan Su, Department of Orthopedics, Xinhua Hospital, Shanghai Jiao Tong University School of Medicine, Shanghai, China. Email: drsujiacan@163.com

Funding information
Foundation of National Center for Translational Medicine (Shanghai) SHU Branch, Grant/Award Number: SUTIM-202303;SUTIM-2023006; National Postdoctoral Researcher Program, Grant/Award Number: GZB20230397; Integrated Project of Major Research Plan of National Natural Science Foundation of China, Grant/Award

Abstract

Osteoporosis (OP) is a systematic bone disease characterized by low bone mass and fragile bone microarchitecture. Conventional treatment for OP has limited efficacy and long-term toxicity. Synthetic biology makes bacterial extracellular vesicle (BEVs)-based therapeutic strategies a promising alternative for the treatment of OP. Here, we constructed a recombinant probiotics *Escherichia coli* Nissle 1917-pET28a-ClyA-BMP-2-CXCR4 (ECN-pClyA-BMP-2-CXCR4), in which BMP-2 and CXCR4 were overexpressed in fusion with BEVs surface protein ClyA. Subsequently, we isolated engineered BEVs-BMP-2-CXCR4 (BEVs-BC) for OP therapy. The engineered BEVs-BC exhibited great bone targeting in vivo. In addition, BEVs-BC had good biocompatibility and remarkable ability to promote osteogenic differentiation of BMSCs. Finally, the synthetic biology-based BEVs-BC significantly prevented the OP in an ovariectomized (OVX) mouse model. In conclusion, we constructed BEVs-BC with both bone-targeting and bone-forming in one-step using synthetic biology, which provides an effective strategy for OP and has great potential for industrialization.

KEYWORDS
bacterial extracellular vesicle, bone targeting, osteogenic differentiation, osteoporosis, synthetic biology

Han Liu, Peiran Song, Hao Zhang, and Fengjin Zhou contributed equally to this work.

Number: 92249303; Shanghai Committee of Science and Technology Laboratory Animal Research Project, Grant/Award Number: 23141900600; National Natural Science Foundation of China, Grant/Award Number: 82202344;82230071; General Program of China Postdoctoral Science Foundation, Grant/Award Number: 2023M732179

1 | INTRODUCTION

Osteoporosis (OP) is a system disease characterized by decreased bone mass, thinning of bone tissue, and increased of bone fragility (Kim et al., 2021; Lee et al., 2021). OP fractures (OPF), the most common complication of OP, have the characteristics of high morbidity, disability, mortality, and high medical expenses, which seriously affect the quality of life of elderly patients (Reid & Billington, 2022). However, the existing biomaterials and conventional methods often have limited effectiveness in the treatment of OP and OPF (Lei et al., 2023). The metabolic imbalance between osteoblasts and osteoclasts often always leads to OP (Song et al., 2022). Several drugs that promote osteoblast activity and inhibit osteoclast resorption have been approved by the U.S. Food and Drug Administration (FDA) (Brown, 2017). However, these drugs have some limitations, including increased risk of cardiovascular adverse reactions, pathological fractures, bone tumours, and immune dysfunction, which severely limit their clinical applications (Khosla, 2009). Therefore, there is an urgent demand for more effective and safer methods for OP treatment.

BMP-2, a well-known growth factor with the ability to promote bone regeneration and increase bone strength and density, is widely used in the treatment of OP and its complications (Park et al., 2013; Segredo-Morales et al., 2018). Due to its short half-life and low retention efficiency, BMP-2 cannot be administered as a stand-alone injection (Chen et al., 2022). However, direct large-scale of administration may cause serious complications. Therefore, advanced biomaterials with controlled release systems are still needed to enable BMP-2 to efficiently promote bone repair. Recently, more and more studies have used extracellular vesicles (EVs) to regulate bone metabolism for the treatment of OP due to the unique nanostructure, stable drug loading capacity, and good biocompatibility of EVs in drug delivery (Huang et al., 2023). Vascular endothelial cells derived EVs could deliver miR-155 to inhibit osteoclast differentiation to improve OP (Song et al., 2019). Engineered NIH-3T3 cells derived EVs can deliver antagomir-188 to promote osteoblast differentiation to alleviate OP (Hu et al., 2021). Moreover, yam-derived EVs could activate bone morphogenetic proteins-2 (BMP-2)/p-p38-dependent Runx2 pathway to prevent OP (Hwang et al., 2023). Although these natural and engineered EVs, including mammalian cells EVs (MEVs) and plants derived EVs (PEVs), have shown excellent therapeutic effect, the complicated engineering modification and low extraction efficiency seriously restrict their clinical applications.

The rapid development of synthetic biology has made the use of bacterial-derived EVs (BEVs) a new star in drug delivery system (Wen et al., 2023). Bacteria have the advantages of large-scale fermentation, rich gene editing approaches, and mature high-density fermentation technology (Liu et al., 2020a, 2020b), which endow BEVs with special characteristics of easy engineering modification and clinical translation (Liu et al., 2023, 2022). BEVs have been reported to regulate bone metabolism and the progression of OP (Han Liu et al., 2022; Liu et al., 2022a). In previous studies, *Escherichia coli* Nissle 1917 (ECN) was modified to overexpress CXCR4, which endowed BEVs with bone-targeting properties (Liu et al., 2023). The bone-targeted bioengineered BEVs-CXCR4 could load and deliver exogenous SOST siRNA to ameliorate OP (Liu et al., 2023). BEVs-CXCR4-SOST siRNA provided an innovative and efficient therapeutic solution for OP. However, low electroporation efficiency seriously hinders their clinical translation process (Alvarez-Erviti et al., 2011). Therefore, it is of great significance to use synthetic biology to construct BEVs with bone-targeting and bone-therapeutic effects in one-step.

In this study, we developed bioengineered BEVs with CXCR4 and BMP-2 in one-step via synthetic biology (Figure 1). We constructed recombinant probiotics ECN-pClyA-BMP-2-CXCR4 to produce bioengineered BEVs-BMP-2-CXCR4 (BEVs-BC), where the BMP-2 and CXCR4 were displayed on the membrane by fusing with ClyA. Furthermore, the therapeutic potential of one-step constructed BEVs-BC was investigated in OVX-induced osteoporotic female mice.

2 | MATERIALS AND METHODS

2.1 | Plasmids and strains

All plasmids and strains constructed in this study are Table 1. The primers used for PCR in this study are listed in Table S1. The sequences of the heterologous BMP-2 and CXCR4 were shown in Tables S2 and S3. pClyA-BMP-2 and pClyA-BMP-2-CXCR4 were constructed using one step cloning kit. The pClyA-BMP-2 were transferred into the chassis cell ECN to obtain the

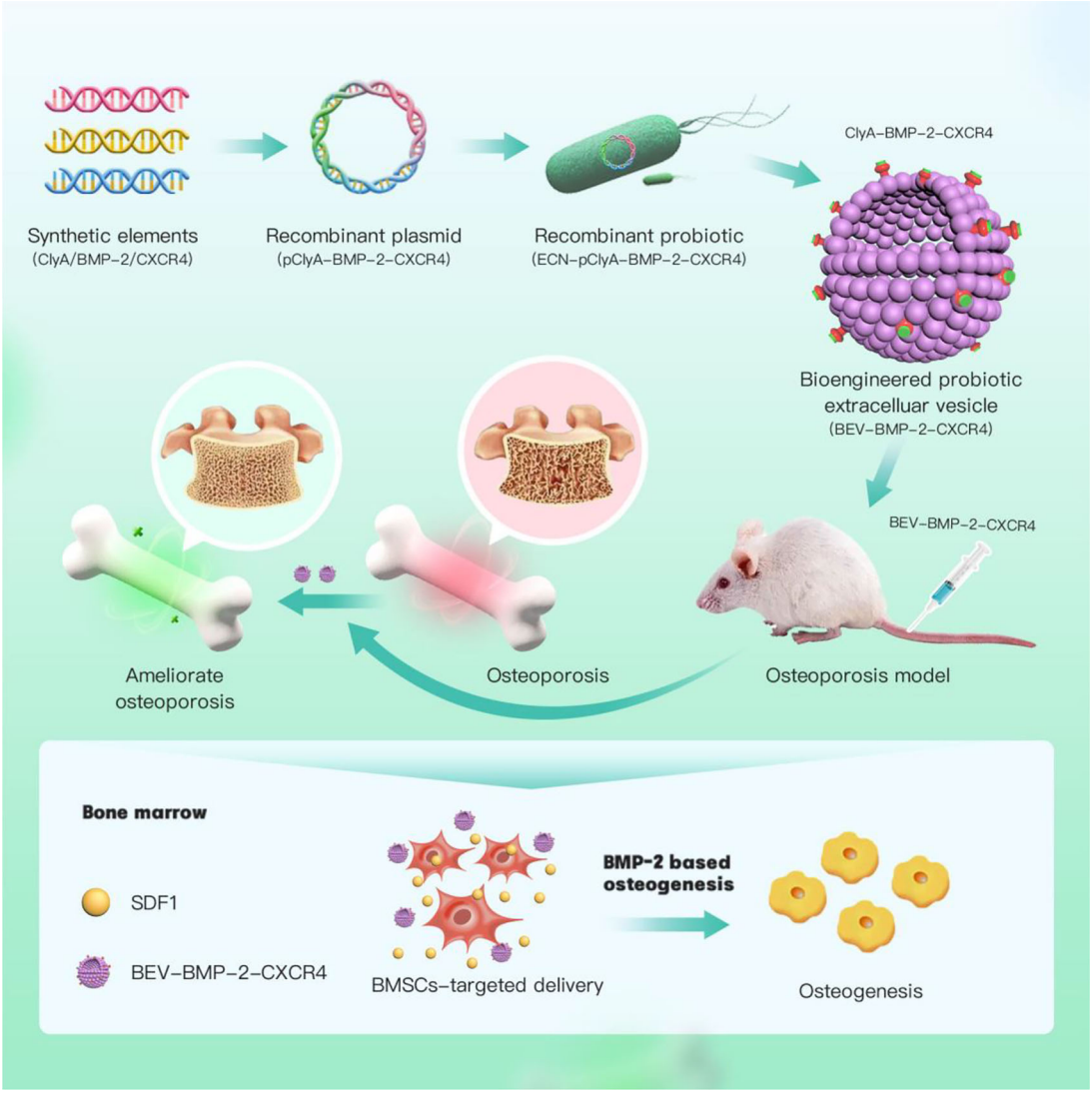

FIGURE 1 The construction and anti-osteoporosis mechanism of bioengineered BEVs. The elements of BMP-2 and CXCR4 were synthesized to construct the recombinant plasmid pClyA-BMP-2-CXCR4, thereby constructing the recombinant probiotic ECN-pClyA-BMP-2-CXCR4. Subsequently, recombinant ECN-pClyA-BMP-2-CXCR4 were cultured to obtain bioengineered BEVs-BC, which could target BMSCs and induce osteogenic differentiation of BMSCs, ultimately improving OP.

TABLE 1 Strains and plasmids used in this study.

Name	Characteristic	Source
Strains		
ECN	*Escherichia coli* Nissle 1917	Lab stock
ECN-pClyA-CXCR4	*Escherichia coli* Nissle 1917 harboring pET28a-ClyA-CXCR4	Liu et al. (2023)
ECN-pClyA-BMP-2	*Escherichia coli* Nissle 1917 harboring pET28a-ClyA-BMP-2	This study
ECN-pClyA-BMP-2-CXCR4	*Escherichia coli* Nissle 1917 harboring pET28a-ClyA-BMP-2-CXCR4	This study
Plasmids		
pET28a	Kan^R	Lab stock
pClyA-CXCR4	Kan^R, pET28a contains ClyA and CXCR4	Liu et al. (2023)
pClyA-BMP-2	Kan^R, pET28a contains ClyA and BMP-2	This study
pClyA-BMP-2-CXCR4	Kan^R, pET28a contains ClyA, BMP-2, and CXCR4	This study

engineered ECN-pClyA-BMP-2, which was used to produce BEVs-BMP-2 (BEVs-B). Similarly, BEVs-BMP-2-CXCR4 (BEVs-BC) and BEVs-CXCR4 (BEVs-C) (Liu et al., 2023) were obtained by the same procedure.

2.2 | Strain culture

LB medium (5 g/L yeast extract, 10 g/L tryptone, and 10 g/L NaCl) was used to cultivate the ECN and recombinant strains. After primary culture (220 rpm, 37°C, 12 h) and secondary culture (220 rpm, 37°C, 8 h), 1 mL of the secondary culture was added into 50 mL of LB for batch culture. Two-step temperature method (37°C for growth and 16°C for protein expression) was performed as previously described (Cheng et al., 2021), which used to efficiently express heterologous BMP-2 and CXCR4.

2.3 | Isolation of BEVs

BEVs were isolated and characterized as previous described (Cheng et al., 2021). To isolate BEVs, bacteria were first removed from 50 mL of fermentation solution by low-speed centrifugation at 10,000 g for 10 min. The filtrate was ultracentrifuged at 150,000 g for 3 h to collect BEVs. The obtained BEVs could be purified again by ultracentrifugation at 150,000 g for 3 h. One millilitre of final collected BEVs can be stored at −80°C. To characterize BEVs, the morphology of BEVs can be observed by transmission electron microscope (TEM; Hitachi, Japan), the particle size and number of BEVs can be obtained by nanoparticle tracking analysis (NTA; NanoSight NS300 UK), and protein contents of BEV can be assessed by BCA protein assay kit (Beyotine, China).

2.4 | Biophotonic imaging analysis

8-week-old C57BL/6 female mice were selected and injected Cy5-labbled BEVs at a dose of 100 μg/100 μL into the tail vein for the in vivo tracer experiments. The mice were executed at 1, 2, and 4 h of injection, and major organs were collected. Fluorescence imaging assays were performed using a Qucikview 3000 machine (Bio-Real Sciences, Austria) to determine the biodistribution of BEVs in mice.

2.5 | Cell cultures

Six-week-old C57s male mice were selected and placed in alcohol for 5 min after cervical dislocation and execution. The skin of the lower limbs of the mice was peeled off under aseptic conditions, excess soft tissues were removed, and the femur was clipped. The bone marrow cavity was then flushed by aspirating the already prepared complete culture medium with a syringe. The rinsed complete medium was collected with a 15 mL centrifuge tube at 1,000*g* and centrifuged for 10 min. After centrifugation, the supernatant was removed, and the precipitate was resuspended with 1 mL of complete medium and then inoculated into cell culture dishes. When the cell fusion rate reaches 70%–80%, the cells can be passaged.

2.6 | Cell viability

BMSCs were plated at a density of 2,000 per well, and the cells were left to attach to the wall. On the second day, 5 μL of BEVs with a nanoparticle number of 10^{12} was added to each well. On the third day, 10 μL of CCK-8 solution was added to each well, and after sufficient mixing without air bubbles, the cells were incubated in a 37°C oven for 1 h. The OD value at 450 nm was detected by using an enzyme labeller to assess cell viability.

2.7 | Western blotting (WB)

Proteins were extracted using protein extraction kit (Beyotine, China). WB was then conducted as previously described (Liu et al., 2023). The gene expression of BMP-2, RUNX2, FABP4, p-SMAD1/5, and SMAD1/5 was detected by WB. Antibodies used for BMP-2 (ab14933; Abcam), CXCR4 (ab124824; Abcam), Runx2 (ab92336; Abcam), FABP4 (ab92501; Abcam), SMAD1/5 (AF5119; Affinity), and P-SMAD1/5 (13820T; CST) were incubated with samples overnight. Secondary antibody (ab6721; Abcam) was added before protein band visualizing.

2.8 | Osteogenic evaluation

The BMSCs were inoculated in 8×10^3 and cultured in a 24-well plate using α-MEM (containing 10% FBS and 1% antibiotics). The medium was then changed to osteogenic induction medium (OriCell, China), and the medium was changed every 2–3 days. After 7 days of cultivation, cells were treated with an ALP kit (Beyotime China) to detect the presence of ALP. After 14 days of cultivation, cells were treated with Alizarin Red S dye (OriCell, China) to detect the presence of calcium nodules.

2.9 | Adipogenic evaluation

The BMSCs were inoculated in 8×10^3 and cultured in a 24-well plate using α-MEM (containing 10%FBS, 1% penicillin and streptomycin). The medium was then changed to lipogenic induction medium (OriCell, China), and the medium was changed every 2–3 days. After 21 days of cultivation, lipid differentiation was detected using oil red O dye (Beyotime China).

2.10 | qRT-PCR analysis

The relative gene expression of Runx2, OSX, OCN, OPN, and Fabp4 was detected by qPCR. The primers for qPCR are listed in Table S1. RNA extraction and RT-PCR assay were conducted as previously described (Liu et al., 2023).

2.11 | Animal and treatments

Female C57BL/6 mice (8-week-old) were selected to construct an ovariectomized (OVX) model in a pathogen-free animal laboratory. Animals were randomly divided into five groups: Sham, OVX, OVX+BEVs-C (BEVs-C), OVX+BEVs-B (BEVs-B), OVX+BEVs-BC (BEVs-BC). For the treatment groups, 0.5 μg protein/μL of BEVs was injected into tail vein once a week for 8 weeks. The cytotoxicity of BEVs was evaluated by H&E staining of heart, liver, spleen, lung, and kidney, as well as the biochemical function of liver and kidney function, including alanine transaminase (ALT), aspartate aminotransferase (AST), blood urea nitrogen (BUN), and creatinine (CREA).

2.12 | Micro-CT analysis

The thigh femurs isolated from the sham and OVX mice were scanned using a Skyscan X-ray microtomography system (Skyscan 1275, Germany). DataViewer, CTAn and CTVox were used to analyse parameters, such as bone mineral density (BMD), bone surface area/total volume (BS/TV), bone volume fraction (BV/TV), and trabecular number (Tb.N).

2.13 | Dynamic histomorphometry analysis

Bone fluorescent-labelling analysis was conducted as previously described (Liu et al., 2023). Briefly, in the 10 days and 3 days before euthanization, 1% calcein was injected into the abdominal cavity successively. The femurs were then placed in 4% paraformaldehyde for light-protected preservation, followed by the preparation of hard tissue sections to detect the formation of green fluorescence. The mineral apposition rate (MAR) was calculated to evaluate the bone-forming ability.

2.14 | H&E staining

H&E staining was performed as previously described (Liu et al., 2023). Briefly, femur samples and major organs were sequentially fixed, decalcified (only for femur samples), embedded, sectioned, and H&E stained. The trabecular area was calculated using Image J (National Institutes of Health, USA).

2.15 | Immunohistochemical staining

Immunohistochemical staining was conducted as previously described (Liu et al., 2023). Briefly, femur samples were sequentially fixed, decalcified, embedded, sectioned, and Immunohistochemical stained (FABP4 antibody).

2.16 | Statistical analysis

All experiments were conducted at least three times. All data are presented as mean ± standard deviation. One-way analysis of variance and *t*-test were performed using GraphPad Prism 9 (GraphPad Software, USA). The value of $P < 0.05$ represent statistically significant.

3 | RESULTS

3.1 | Characterization of bioengineered BEVs-BC

In our previous study, we constructed a recombinant probiotic ECN-pClyA-CXCR4 to obtain bone-targeted bioengineered BEVs-C (Liu et al., 2023). To obtain bioengineered BEVs with bone-targeting and bone-therapeutic capabilities, the elements of BMP-2 and CXCR4 were synthesized to construct the recombinant plasmid pClyA-BMP-2 (Figures 2a, b, and S1) and pClyA-BMP-2-CXCR4 (Figures 2a, b, and S2), thereby constructing the recombinant probiotic ECN-pClyA-BMP-2 and ECN-pClyA-BMP-2-CXCR4. For better heterologous protein expression, a two-stage temperature method was used for the cultivation of recombinant probiotics (Figure 2c). 0.1 mM IPTG was added to induce BMP-2 and BMP-2-CXCR4 protein expression when OD_{600} reached at 0.6 (Figure 2d, red arrow). Compared to expression of one heterologous protein, simultaneous expression of two heterologous proteins did not affect bacterial growth (Figure 2d), which made it possible to simultaneously endow BEVs with bone-targeting and bone-healing abilities.

Subsequently, bioengineered BEVs-B and BEVs-BC were isolated from multiple ultracentrifugation. As shown in Figure 2(e, f), the TEM images showed that the morphology of BEVs-B and BEVs-BC were typical spherical morphology. In our previous study, we have constructed engineered BEVs-C where CXCR4 was overexpressed on the membrane surface of BEVs using ClyA-based Plug-and-Display technology (Liu et al., 2023). Similarly, we also constructed BEVs-B expressing BMP-2 on the membrane surface and BEVs-BC expressing both BMP-2 and CXCR4 on the membrane surface (Figure 2g). In addition, the results of NTA showed that the size of the BEVs-B and BEVs-BC were 165.8 and 170.6 nm, respectively (Figure 2h, i). In addition, the concentration of the BEVs-B and BEVs-BC were 2.5×10^{11} particles/mL and 3.8×10^{11} particles/mL, respectively (Figure 2h, i). Moreover, the results of BCA showed that the protein contents of the BEVs-B and BEVs-BC were 0.40 and 0.46 mg/mL, respectively. Taken together, we successfully developed bioengineered BEVs-BC with expression of BMP-2 and CXCR4 on the membrane surface.

3.2 | in vivo distribution of BEVs-BC

The significance of targeted therapy lies in increased local drug concentration and reduced side effects (Liang et al., 2021). Our team also proposed the concept of bone-targeted biomaterial strategy for osteoporotic bone repair (Ren et al., 2022). Natural or engineered EVs exhibit strong bone-targeting capabilities and become promising therapeutic approaches for orthopaedic diseases (Wang et al., 2023). Although we have verified the great in vivo targeting ability of $CXCR4^+$ BEVs (Liu et al., 2023) and $CXCR4^+$ MEVs (Hu et al., 2021), we further investigated the in vivo distribution of BEVs-BC in the presence of BMP-2 expression.

The bone accumulation of BEVs-BC was evaluated using biophotonic imaging after injection of Cy5-labeled BEVs into mice. The heart, liver, spleen, lungs, kidneys, and femur were obtained for biophotonic imaging. The femur was used as a representative bone for analysis. A stronger fluorescent intensity was observed in the femur of BEVs-BC treated mice 4 h after injection (Figure 3a and Figure S3). Moreover, there was a progressive elevation observed in the fluorescence intensity within the femur from 1 to 4 h after injection (Figure 3b). These results revealed that BEVs-BC may efficiently accumulate in bone tissue and reduce their distribution in other organs. In conclusion, BEVs-BC exhibited a strong bone-targeting ability in vivo, which provided the possibility for subsequent highly effective treatment.

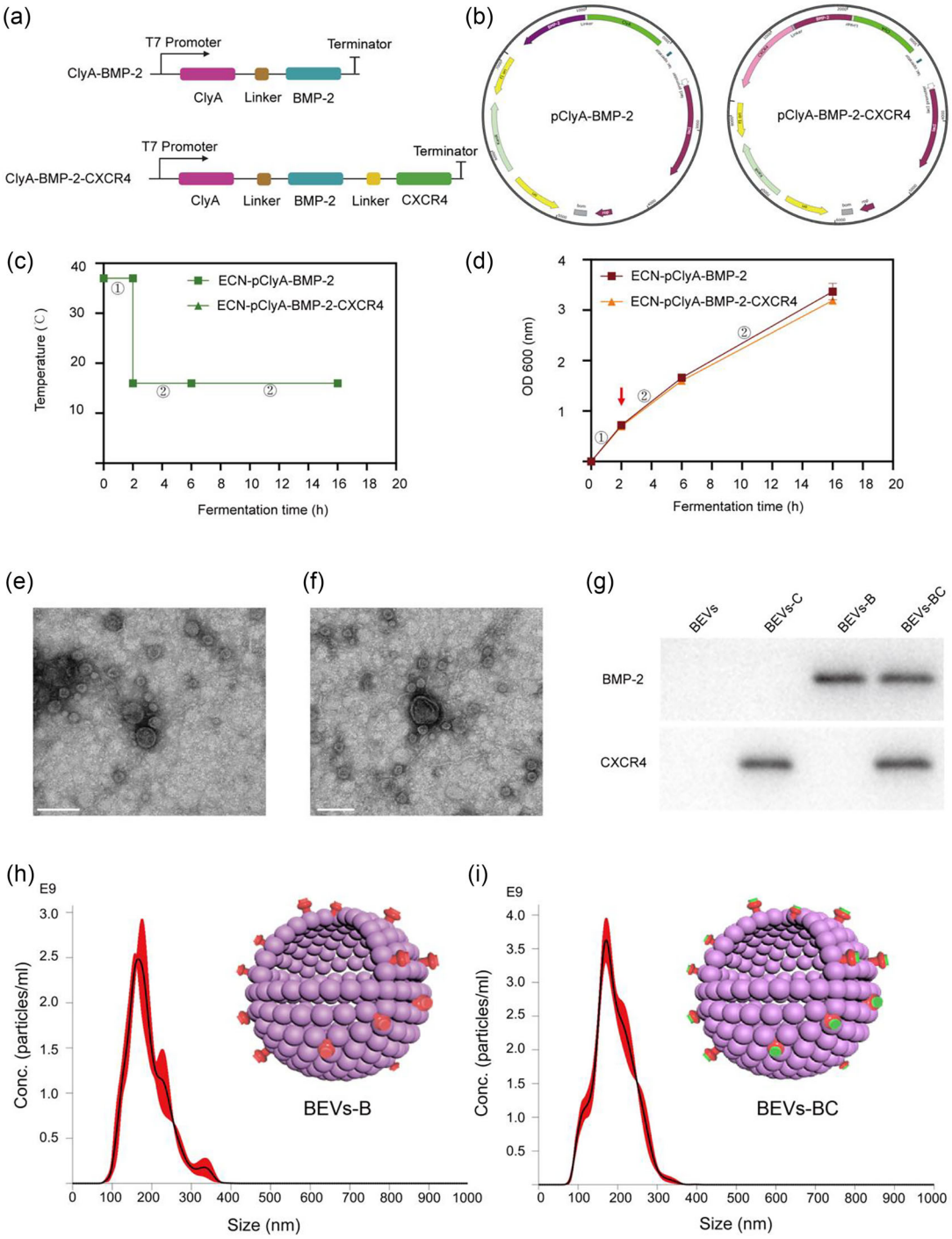

FIGURE 2 Design and characterization of bioengineered BEVs. (a) Schematic illustration of the construct used to express ClyA-BMP-2 and ClyA-BMP-2-CXCR4. (b) Schematic illustration of the pClyA-BMP-2 and pClyA-BMP-2-CXCR4 construct. (c) Schematic diagram of the two-stage temperature culture for ECN-pClyA-BMP-2 and ECN-pClyA-BMP-2-CXCR4. (d) The growth of ECN-pClyA-BMP-2 and ECN-pClyA-BMP-2-CXCR4. (e) TEM images of BEVs-B. Scale bars represent 100 μm. (f) TEM images of BEVs-BC. Scale bars represent 100 μm. (g) Western blot analysis of the expression of BMP-2 in BEVs-B and the expressions of BMP-2 and CXCR4 in BEVs-BC. (h) NTA results of BEVs-B. (I) NTA results of BEVs-BC, the red colour represents BMP-2 and green colour represents CXCR4.

3.3 | BEVs-BC promote osteogenic differentiation and inhibit adipogenic differentiation of BMSCs in vitro

Cell viability was checked using a calcein-AM/propidium iodide (PI) kit. As shown in Figure 4(a), compared with the PBS group, the experimental group (including BEVs-C, BEVs-B, and BEVs-BC group) did not produce obvious cytotoxicity against BMSCs.

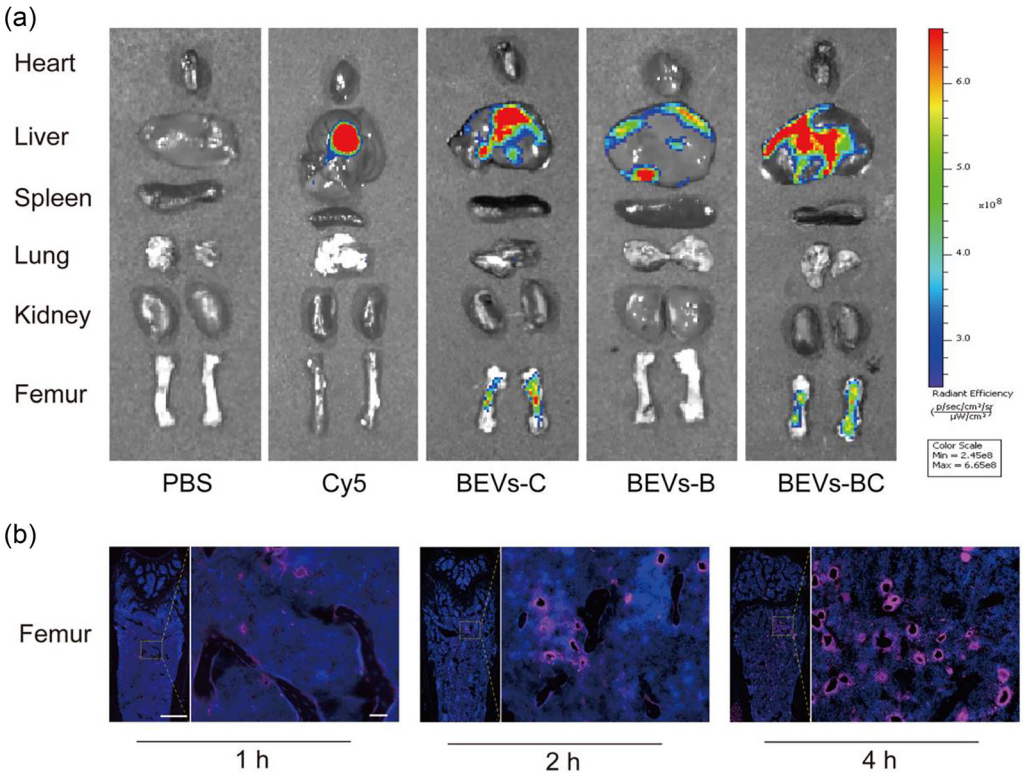

FIGURE 3 in vivo distribution of BEVs-BC. (a) in vivo biodistribution of Cy5-labelled BEVs-C, BEVs-B, and BEVs-BC 4 h after injection, $n = 3$. (b) Representative fluorescence microscopic images of the femur in 1, 2, and 4 h after injection of Cy5-labeled BEVs-CSs, $n = 3$. Scale bar on femur represent 500 μm (left) and 50 μm (right).

Moreover, cytocompatibility of BEVs-BC was also evaluated using CCK-8 Kit. As shown in Figure 4(b), no obvious cytotoxicity of BEVs-BC to bone marrow mesenchymal stem cells (BMSCs) ranging from 0 to 100 μg/mL was found. It could be seen that BEVs-BC had no obvious effect on cell proliferation, which confirmed the safety and cytocompatibility of BEVs-BC at the cellular level.

Subsequently, the effect of BEVs-BC on the osteogenic differentiation of BMSCs was further examined. Alkaline Phosphatase (ALP, early osteogenic differentiation) and Alizarin red staining (ARS, late osteogenic differentiation) were performed to assess osteogenic performance. Compared with PBS groups, BEVs-C and BEVs-B group had higher ALP activity (Figure 4c, d) as well as more obvious mineralized nodules (Figure 4e, f). Compared with the BEVs-B group, the BEVs-BCs group, including the bone-targeting and bone-healing abilities, had slightly higher ALP activity (Figure 4c, d), but there was no obvious difference in mineralized nodules (Figure 4e, f). In addition, it has been reported that the abnormal osteogenic differentiation and adipogenic differentiation of BMSCs also results in OP (Zeng & Xie, 2022). Oil Red O staining was conducted to evaluate the adipogenic differentiation. As shown in Figure 4(g, h), BEVs-C slightly inhibited the formation of lipid drops in BMSCs, while BEVs-B and BEVs-BC significantly inhibited lipid drops formation in BMSCs.

The expression of osteogenic-related gene, including Runx2, OCN, OSX, and OPN, was assessed through qRT-PCR and WB. BEVs-C, BEVs-B, and BEVs-BC group had higher relative Runx2 mRNA expression than that of PBS group (Figure 5a). The trend of the relative mRNA expression of OSX, OCN, and OPN was consistent with the results of osteogenic staining (Figure 5b, c, d). Moreover, the protein expression of Runx2 was also consistent with the results of ALP/ARS and qPCR (Figure 5e and Figure S4). Similarly, the qRT-PCR and WB were also used for evaluating the expression of adipogenic-related gene, such as fatty acid binding protein 4 (Fabp4). The relative mRNA level and protein level of Fabp4 decreased significantly when treated with BEVs-B and BEVs-BC (Figure 5f, h, and Figure S5). Generally, these results demonstrated that BEVs-BCs could effectively promote osteogenic differentiation and inhibit adipogenic differentiation of BMSCs in vitro.

3.4 | BEVs-BC improve osteoporosis by activating BMP/SMAD signalling pathway

After the successful in vitro verification of the BEVs-BC, the OVX model was used for further investigation in vivo. PBS, BEVs-C, BEVs-B, and BEVs-BC were injected into tail vein to treat OVX mice. Tail vein injections were performed once a week and

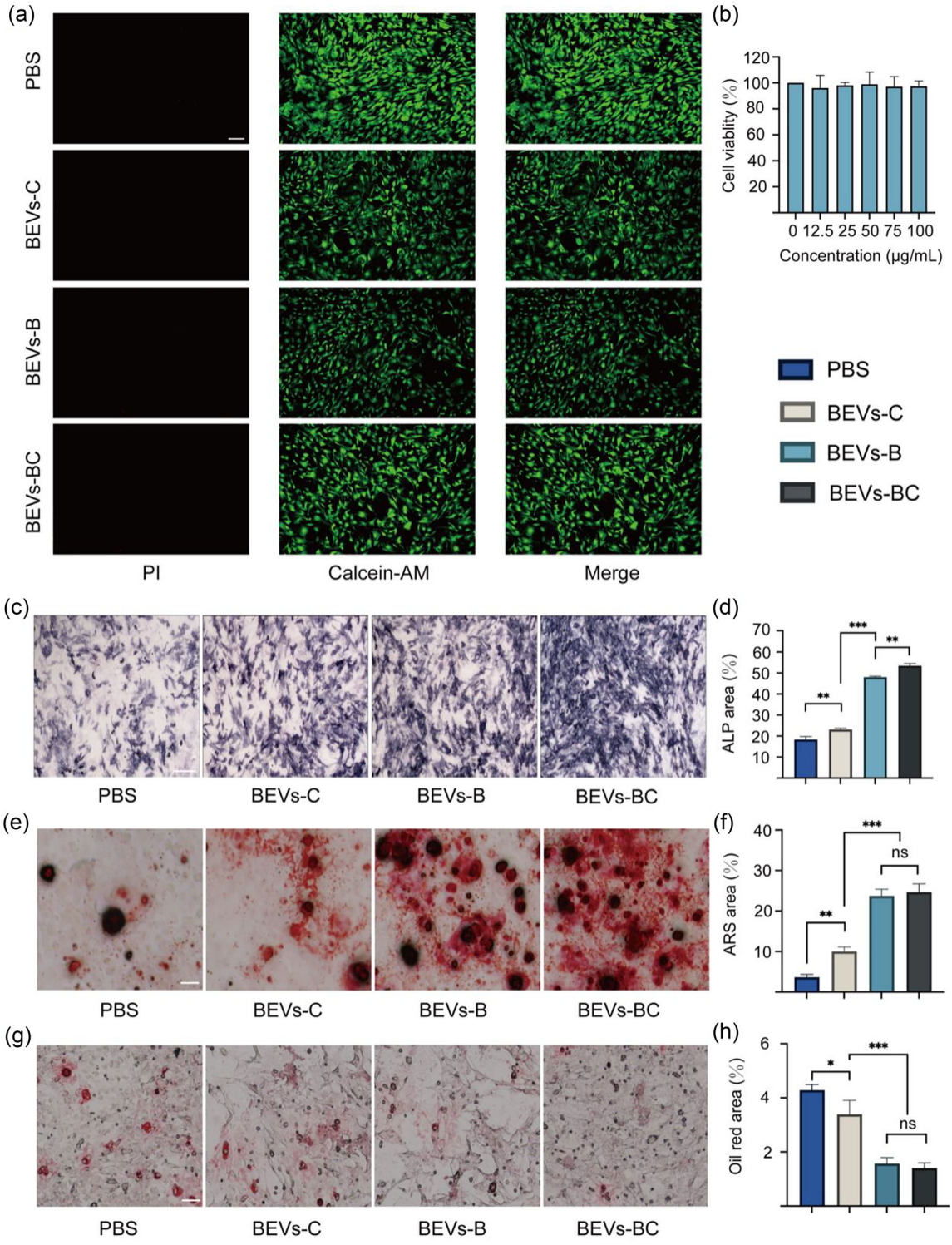

FIGURE 4 BEVs-BC promote osteogenic differentiation and inhibit adipogenic differentiation of BMSCs in vitro. (a) Representative D/L staining of BMSCs with PBS, BEVs-C, BEVs-B, and BEVs-BC, $n = 3$. (b) The potential cytoxicity of BEVs-CSs in vitro, n = 6. (c) Representative ALP staining of BMSCs after treating with PBS, BEVs-C, BEVs-B, and BEVs-BC, $n = 3$. Scale bars represent 250 μm. (d) Quantification of ALP staining. (e) Representative ARS staining of BMSCs after treating with PBS, BEVs-C, BEVs-B, and BEVs-BC, $n = 3$. Scale bars represent 100 μm. (f) Quantitative analysis of ARS staining. (g) Representative Oil Red O staining of BMSCs after treating with PBS, BEVs-C, BEVs-B, and BEVs-BC, $n = 3$. Scale bars represent 100 μm. (h) Quantitative analysis of Oil Red O staining. $^{*}P < 0.05$, $^{**}P < 0.01$, $^{***}P < 0.001$.

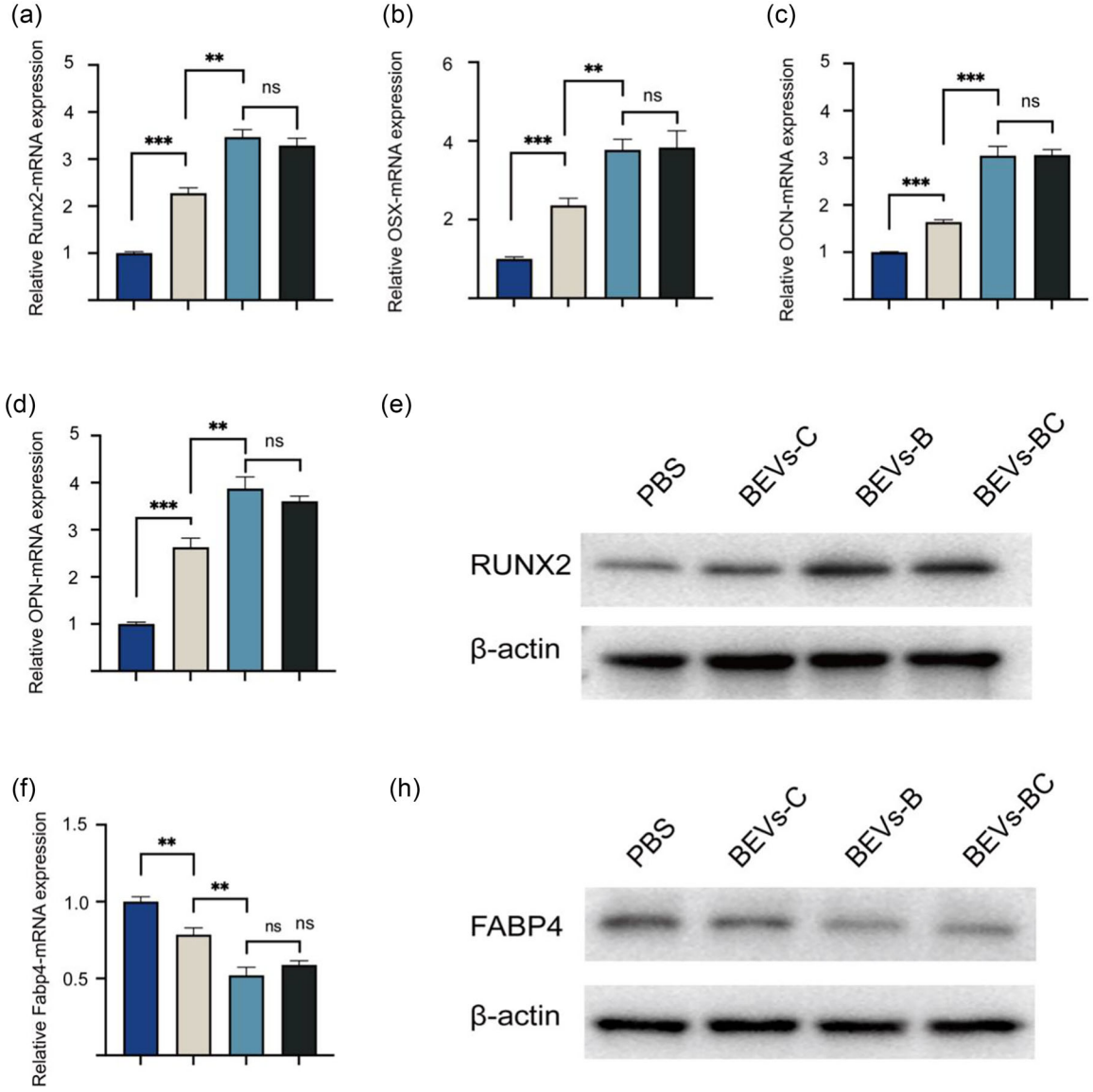

FIGURE 5 qRT-PCR and WB were used for assessing the expression of osteogenic- and adipogenic related gene. (a) The relative mRNA expression of Runx2, $n = 3$. (b) The relative mRNA expression of OSX, $n = 3$. (c) The relative mRNA expression of OCN, $n = 3$. (d) The relative mRNA expression of OPN, $n = 3$. (e) WB assay of Runx2. (f) The relative mRNA expression of Fabp4, $n = 3$. (g) WB assay of FABP4. $^{*}P < 0.05$, $^{**}P < 0.01$, $^{***}P < 0.001$.

samples were taken for subsequent analysis after 8 weeks. The bone microarchitecture of the distal femur was analysed by micro-CT (Song et al., 2019). Compared with the OVX group, the BEVs-B, BEVs-C, and BEVs-BC group showed better bone microarchitecture (Figure 6a) and better BMD, BV/TV, BS/TV and Tb.N (Figure 6b). Moreover, dynamic bone formation was also analysed by calcein double labelling experiments (Guo et al., 2023). The BEVs-B, BEVs-C, and BEVs-BC group also have better bone formation rate, represented by width of the green fluorescence, than that of OVX group (Figure 6c, d).

To further evaluate the bone formation ability of BEVs-BC, bone histomorphological analysis, such as H&E staining and immumohistochemical staining, was also conducted. H&E staining confirmed that the trabecular bone number was significantly increased in the BEVs-BC group compared with other treatment groups (Figure 6e, f). Moreover, immunohistochemical (IHC) staining of Fabp4 was used to examine the adipogenic differentiation of BMSCs. As expected, the group of BEVs-BC effectively decreased the quantity of bone marrow adipocytes in comparison to other treatment groups (Figure 6h, i). We demonstrated that BEVs-B had a strong osteogenic effect in vitro experiment, however, this effect could be amplified by the targeting function in vivo. In conclusion, the constructed bioengineered BEVs-BC displaying BMP-2 to BMSCs and improve bone loss via promoting osteogenic differentiation and inhibiting adipogenic differentiation of BMSCs.

The BMP/SMAD signalling pathway is a vital signalling pathway in osteoblast differentiation and osteoblast mineralization (Wu et al., 2016; Xu et al., 2021). The loss of BMP-SMAD signalling significantly blocks the expression of Runx2 and leads to

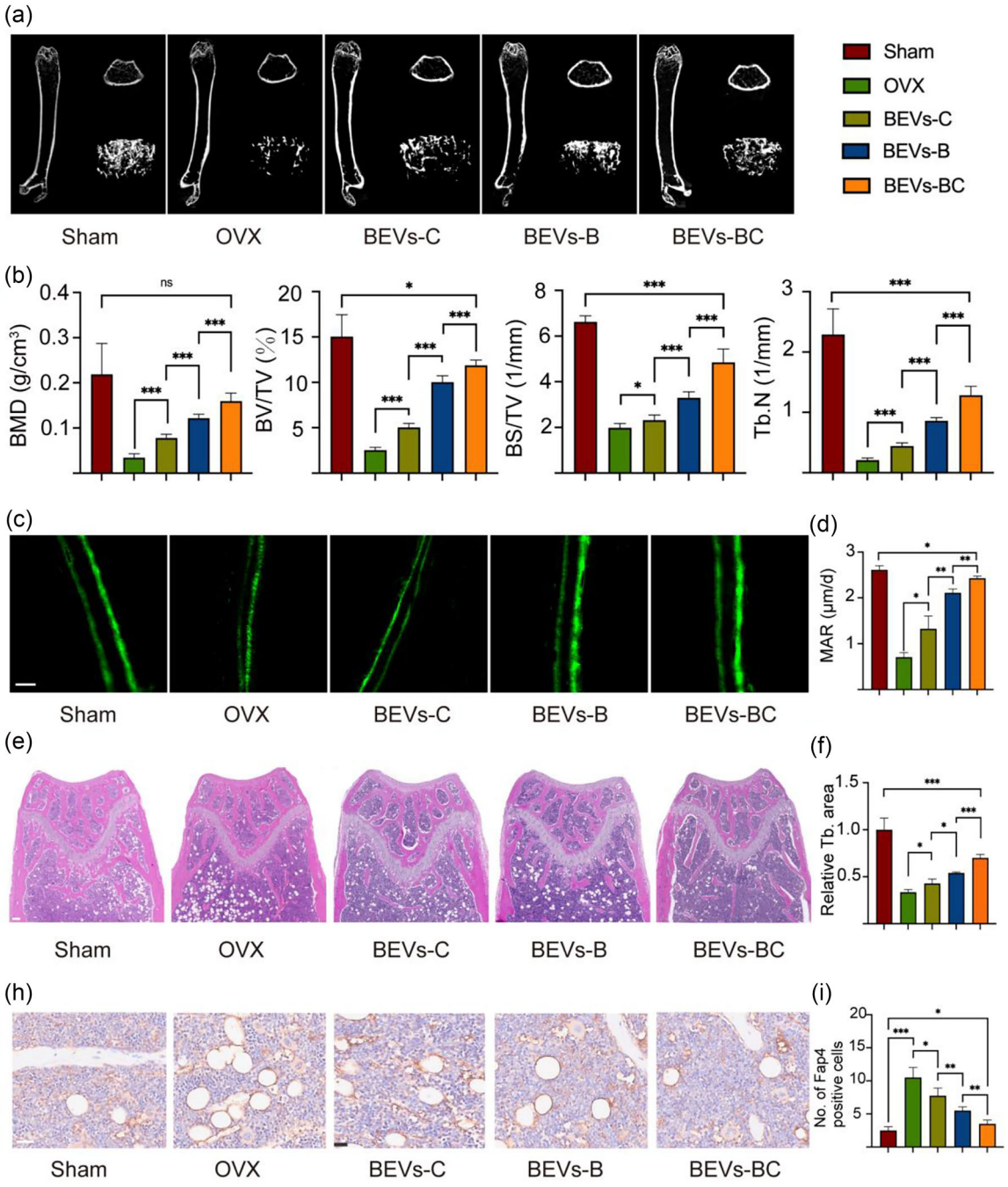

FIGURE 6 BEVs-BC ameliorate osteoporosis in vivo. (a) Representative Micro-CT images of the distal femur. (b) Quantitative analysis of BMD, BV/TV, BS/TV, and Tb. *N*, respectively, $n = 6$. (c) Representative calcein double-labeling assay. scale bar = 20 μm. (d) Quantitative analysis of MAR, $n = 6$. (e) Representative H&E staining of distal femur sections, $n = 6$. Scale bar = 200 μm. (f) Quantitative analysis of trabecular bone area. (h) Representative immunohistochemistry staining of FABP4 of the distal femora, $n = 6$. scale bar = 50 μm. (i) Quantification of FABP4 positive cells. $^{*}P < 0.05$, $^{**}P < 0.01$, $^{***}P < 0.001$.

decreased bone formation (Fan et al., 2021). To further investigate the regulation of the BMP/SMAD signalling pathway, the expression level of SMAD5, phosphorylated SMAD5 (p-SMAD5) and BMP-2 was measured in BEVs and BEVs-BC groups. The WB results showed that there is almost no change of SMAD5 in the BEVs and BEVs-BC groups (Figure 7a and Figure S6). However, compared with the BEVs group, the expressions of p-SMAD5 and BMP-2 were significantly enhanced in the BEVs-BC group (Figure 7b and Figure S7). These results suggested that bioengineered BEVs-BC promoted osteogenic differentiation of BMSCs by activating the BMP-SMAD signalling pathway. The schematic diagram of the BMP/SMAD signalling pathway activated by BMP-2 is shown in Figure 7(c).

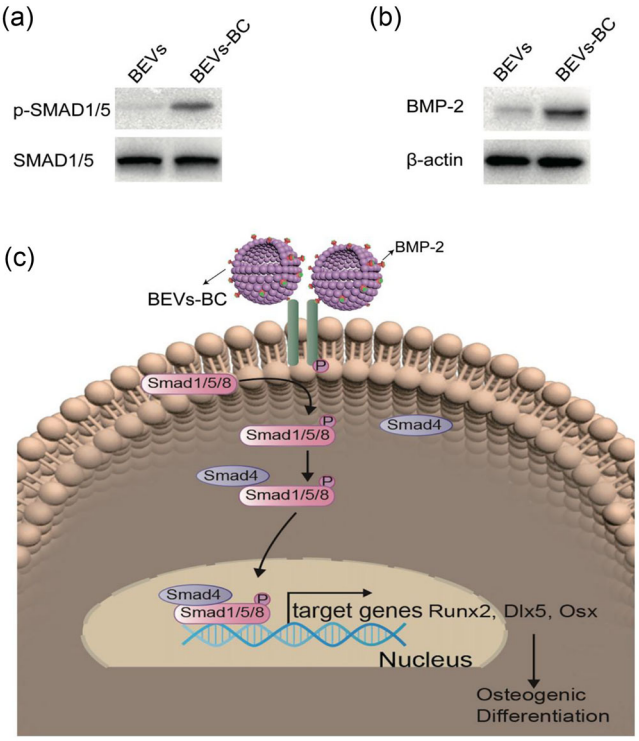

FIGURE 7 BEVs-BC promote chondrogenic differentiation by activating SMAD5 signalling. (a) The expression of SMAD5 and p-SMAD5 proteins after BEVs and BEVs-BC treatment. (b) The expression of BMP-2 proteins after BEVs and BEVs-BC treatment. (c) Schematic diagram of the signalling pathways. $^{*}P < 0.05$, $^{**}P < 0.01$, $^{***}P < 0.001$.

3.5 | in vivo toxicity assay of BEVs

As cell-free nanocarriers, BEVs have been shown to be safe by numerous studies and are unlikely to cause chronic systemic toxicity or other side effects (Cheng et al., 2021; Gujrati et al., 2019; Li et al., 2020; Thomas et al., 2022). Here, the long-term cytotoxicity of engineered BEVs was also evaluated in vivo after intravenous injection. As shown in Figure 8(a), no significant changes were observed in the major organs after 8 weeks of administration. Moreover, there was also no significant difference in liver and kidney function, such as ALT, AST, BUN, and CREA, after administration of BEVs-BC for 8 weeks (Figure 8b). Taken together, these results suggested that such synthetic biology-based bioengineered BEVs-BC had an excellent in vivo biosafety and are expected to be targeted drug nanocarriers for clinical applications.

4 | DISCUSSION

OP is mainly caused by the imbalance of bone-forming and bone-resorbing (Guo et al., 2023). Despite the widely applied anti-resorptive agents (such as bisphosphonates (Rachner et al., 2011) and denosumab (Bone et al., 2017) and anabolic drugs (such as parathyroid hormone (Neer et al., 2001), innovative treatment strategy to regulate the osteoblasts-osteoclasts balance are emphasized (Zhou et al., 2021). Recently, the influence of gut microbes on bone metabolism has received increasing attention (Lyu et al., 2023). Microbes could affect human health by influencing symbiotic flora to inhibit pathogens, regulating host immune responses, increasing epithelial barrier function, and enhancing tight junction function, which are considered to be the first generation of the gut-bone axis (Zaiss et al., 2019).

Moreover, BEVs-based gut-bone axis, also named the second-generation gut-bone axis, has gradually shown its strong potential (Chen et al., 2022; Liu et al., 2022c, 2022d). The modification of BEVs includes engineering parental strains to generate functional BEVs and engineering BEVs after isolation (Cheng & Hill, 2022). It is easier to obtain more BEVs directly by constructing recombinant strains based on synthetic biology to produce functional BEVs than that of engineering BEVs after isolation. Therefore, we constructed a BEV with bone-targeting protein CXCR4 and bone-therapeutic protein BMP-2 on the membrane surface in one-step through synthetic biology. This easily customizable and available BEVs-BC could target BMSCs in the bone marrow, thereby promoting osteogenic differentiation via BMP/SMAD signalling pathway, ultimately improving OVX-induced bone loss.

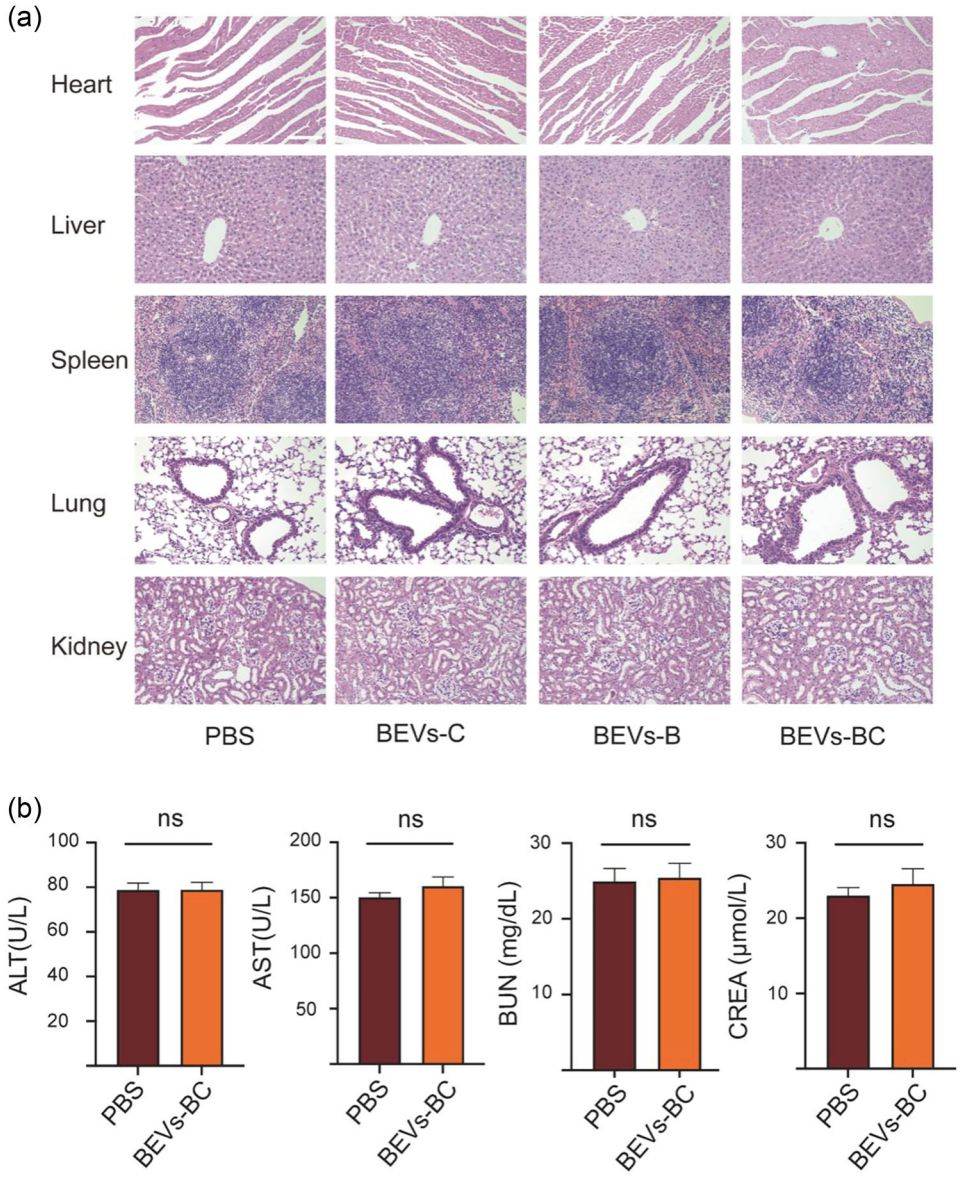

FIGURE 8 in vivo toxicity assay of bioengineered BEVs. (a) H&E staining of the heart, liver, spleen, lung, and kidney after administration of PBS, BEVs-C, BEVs-B, and BEVs-BC, $n = 3$. Scale bar = 100 μm. (b) Toxicity test of alanine transaminase (ALT), aspartate aminotransferase (AST), blood urea nitrogen (BUN), and creatinine (CREA), $n = 3$. $^{*}P < 0.05$, $^{**}P < 0.01$, $^{***}P < 0.001$.

In our previous studies, we electroporated SOST siRNA on the basis of BEVs-C for the treatment of OP (Liu et al., 2023). However, the electroporation efficiency is only about 20%. Although BEVs-CSs is an innovative and effective therapeutic drug, inefficient electroporation will consume a large amount of expensive siRNA, which will also affect the further mass production and clinical transformation of BEVs. However, synthetic biology technology allows probiotic ECN to heterologous overexpress BMP-2 on the membrane surface. Moreover, BEVs containing BMP-2 can be obtained in large quantities through a simple two-stage temperature fermentation. The construction time and cost of BEVs-BC are greatly shortened compared with that of BEVs-CSs. In addition, in terms of transformation methods, BEVs-BC could be obtained directly without modifying the separated BEVs. Obtaining BEVs-CSs requires modifying the parent strain and then modifying the isolated BEVs-C, which undoubtedly increases the time for material construction. Therefore, for BEVs-BC, we created a new bone repair material with a simple construction method, easy access, and powerful functions, laying the foundation for future clinical translation.

Currently, EVs can be divided into BEVs, MEVs, and EVs from plants (Cong et al., 2022). We have also defined organoid-derived EVs as OEVs, a type of three-dimensionally cultured MEVs, and proposed the concept of a third-generation gut-bone axis, which could regulate bone metabolism based on intestinal OEVs (Liu et al., 2023, Liu & Su, 2023). In addition, PEVs have also begun to be applied to the regulation of bone metabolism. Hwang et al. (2023) applied yam-derived PEVs to stimulate osteoblast formation and prevent osteoporosis in mice. Taken together, EVs have become a shining star in nanomedicine

(Wu et al., 2021). The advantages of BEVs include their ease of modification and industrialization. The rapid development of synthetic biology also endows BEVs with great potential, which paves a bright path for the application of BEVs.

Herein, we provided an intravenous injection for the treatment of OP. In general, the treatment of systemic diseases based on BEVs relies on intravenous injection (Chen et al., 2020). However, oral administration is a safer treatment with good patient compliance and economics compared with intravenous injection. (Yue et al. 2022) developed a BEVs-based oral bacteria strategy. Oral administration of engineered bacteria and arabinose (promoter inducer) could controllably induce the bacteria to produce functional BEVs with target antigens in the intestine for the regulation of immunity. In our future study, adopting BEVs-based oral bacterial strategies to deliver stimulatory molecules to regulate immune cells, such as Th17/Treg cell balance (Fu et al., 2022), is an extremely promising direction for OP therapy.

5 | CONCLUSIONS

In this work, we developed a recombinant probiotic ECN-pClyA-BMP-2-CXCR4 by synthetic biology. After a simple fermentation and purification, we could obtain large-scale bioengineered BEVs-BC with bone-targeting and bone-therapeutic properties. This bioengineered BEVs-BC could target BMSCs in bone marrow, thereby promoting osteogenic differentiation and inhibiting their adipogenic differentiation via BMP/SMAD signalling pathway, ultimately improving OVX-induced bone loss. Our study further demonstrated that the potential of BEVs, especially probiotic EVs, in bone degenerative diseases, providing an innovative solution for OP therapy. Importantly, we have developed a readily available and powerful bone repair biomaterial, laying a solid foundation for future clinical applications.

AUTHOR CONTRIBUTIONS

Han Liu: Conceptualization; data curation; formal analysis; methodology; validation; visualization; writing—original draft. **Peiran Song**: Conceptualization; data curation; formal analysis; funding acquisition; resources; validation. **Hao Zhang**: Formal analysis; validation; visualization. **Fengjin Zhou**: Formal analysis; visualization. **Ning Ji**: Data curation; formal analysis. **Mingkai Wang**: Data curation; formal analysis. **Guangyin Zhou**: Data curation; formal analysis. **Ruina Han**: Data curation; formal analysis. **Xinru Liu**: Data curation; formal analysis. **Weizong Weng**: Data curation; formal analysis. **Haoqi Tan**: Data curation; formal analysis. **Sicheng Wang**: Resources; supervision; writing—review and editing. **Lei Zheng**: Project administration; resources; supervision; writing—review and editing. **Yingying Jing**: Funding acquisition; project administration; resources; supervision; writing—review and editing. **Jiacan Su**: Funding acquisition; project administration; resources; supervision; writing—review and editing.

ACKNOWLEDGEMENTS

This work was supported by the National Natural Science Foundation of China (82230071, 82202344); Integrated Project of Major Research Plan of National Natural Science Foundation of China (92249303); Shanghai Committee of Science and Technology Laboratory Animal Research Project (23141900600, 21140904900); Foundation of National Centre for Translational Medicine (Shanghai) SHU Branch (SUTIM-202303, SUTIM-2023006); General Program of China Postdoctoral Science Foundation (2023M732179); National Postdoctoral Researcher Program (GZB20230397). We thank Echo Biotech Co., Ltd at Beijing, P. R. China for providing excellent technical assistance and for BEVs purification and characterisation service.

CONFLICT OF INTEREST STATEMENT

The authors declare they have no conflict of interest.

DATA AVAILABILITY STATEMENT

The data that support the findings of this study are available from the corresponding author upon reasonable request.

ORCID

Lei Zheng https://orcid.org/0000-0003-2576-8780
Jiacan Su https://orcid.org/0000-0001-7080-263X

REFERENCES

Kim, H. Y., Song, M. K., Gho, Y. S., Kim, H. H., & Choi, B. K. (2021). Extracellular vesicles derived from the periodontal pathogen Filifactor alocis induce systemic bone loss through Toll-like receptor 2. *Journal of Extracellular Vesicles*, *10*(12), e12157. https://doi.org/10.1002/jev2.12157

Lee, K. S., Lee, J., Kim, H. K., Yeom, S. H., Woo, C. H., Jung, Y. J., Yun, Y. E., Park, S. Y., Han, J., Kim, E., Sul, J. H., Jung, J. M., Park, J. H., Choi, J. S., Cho, Y. W., & Jo, D.-G. (2021). Extracellular vesicles from adipose tissue-derived stem cells alleviate osteoporosis through osteoprotegerin and miR-21-5p. *Journal of Extracellular Vesicles*, *10*(12), e12152. https://doi.org/10.1002/jev2.12152

Reid, I. R., & Billington, E. O. (2022). Drug therapy for osteoporosis in older adults. *Lancet*, *399*(10329), 1080–1092. https://doi.org/10.1016/s0140-6736(21)02646-5

Lei, C., Song, J. H., Li, S., Zhu, Y. N., Liu, M. Y., Wan, M. C., Mu, Z., Tay, F. R., & Niu, L. N. (2023). Advances in materials-based therapeutic strategies against osteoporosis. *Biomaterials*, *296*, 122066. https://doi.org/10.1016/j.biomaterials.2023.122066

Song, S., Guo, Y., Yang, Y., & Fu, D. (2022). Advances in pathogenesis and therapeutic strategies for osteoporosis. *Pharmacology & Therapeutics*, *237*, 108168. https://doi.org/10.1016/j.pharmthera.2022.108168

Brown, C. (2017). Osteoporosis: Staying strong. *Nature*, *550*(7674), S15–s17. https://doi.org/10.1038/550S15a

Khosla, S. (2009). Increasing options for the treatment of osteoporosis. *New England Journal of Medicine*, *361*(8), 818–820. https://doi.org/10.1056/NEJMe0905480

Segredo-Morales, E., García-García, P., Reyes, R., Pérez-Herrero, E., Delgado, A., & Évora, C. (2018). Bone regeneration in osteoporosis by delivery BMP-2 and PRGF from tetronic-alginate composite thermogel. *International Journal of Pharmacy*, *543*(1-2), 160–168. https://doi.org/10.1016/j.ijpharm.2018.03.034

Park, S. B., Park, S. H., Kim, N. H., & Chung, C. K. (2013). BMP-2 induced early bone formation in spine fusion using rat ovariectomy osteoporosis model. *Spine Journal*, *13*(10), 1273–1280. https://doi.org/10.1016/j.spinee.2013.06.010

Chen, X., Wang, S., Zhang, X., Yu, Y., Wang, J., & Liu, C. (2022). Dual-function injectable fibrin gel incorporated with sulfated chitosan nanoparticles for rhBMP-2-induced bone regeneration. *Applied Materials Today*, *26*, 101347. https://doi.org/10.1016/j.apmt.2021.101347

Huang, R., Jia, B., Su, D., Li, M., Xu, Z., He, C., Huang, Y., Fan, H., Chen, H., & Cheng, F. (2023). Plant exosomes fused with engineered mesenchymal stem cell-derived nanovesicles for synergistic therapy of autoimmune skin disorders. *Journal of Extracellular Vesicles*, *12*(10), e12361. https://doi.org/10.1002/jev2.12361

Song, H., Li, X., Zhao, Z., Qian, J., Wang, Y., Cui, J., Weng, W., Cao, L., Chen, X., Hu, Y., & Su, J. (2019). Reversal of osteoporotic activity by endothelial cell-secreted bone targeting and biocompatible exosomes. *Nano Letters*, *19*(5), 3040–3048. https://doi.org/10.1021/acs.nanolett.9b00287

Hu, Y., Li, X., Zhang, Q., Gu, Z., Luo, Y., Guo, J., Wang, X., Jing, Y., Chen, X., & Su, J. (2021). Exosome-guided bone targeted delivery of Antagomir-188 as an anabolic therapy for bone loss. *Bioactive Materials*, *6*(9), 2905–2913. https://doi.org/10.1016/j.bioactmat.2021.02.014

Hwang, J.-H., Park, Y.-S., Kim, H.-S., Kim, D.-h., Lee, S.-H., Lee, C.-H., Lee, S.-H., Kim, J.-E., Lee, S., Kim, H. M., Kim, H.-W., Kim, J., Seo, W., Kwon, H.-J., Song, B.-J., Kim, D.-K., Baek, M.-C., & Cho, Y.-E. (2023). Yam-derived exosome-like nanovesicles stimulate osteoblast formation and prevent osteoporosis in mice. *Journal of Controlled Release*, *355*, 184–198. https://doi.org/10.1016/j.jconrel.2023.01.071

Wen, M., Wang, J., Ou, Z., Nie, G., Chen, Y., Li, M., Wu, Z., Xiong, S., Zhou, H., Yang, Z., Long, G., Su, J., Liu, H., Jing, Y., Wen, Z., Fu, Y., Zhou, T., Xie, H., Guan, W., … Zheng, L. (2023). Bacterial extracellular vesicles: A position paper by the microbial vesicles task force of the Chinese society for extracellular vesicles. *Interdisciplinary Medicine*, *1*(3), e20230017. https://doi.org/10.1002/INMD.20230017

Liu, H., Wang, Y., Hou, Y., & Li, Z. (2020a). Fitness of chassis cells and metabolic pathways for l-cysteine overproduction in *Escherichia coli*. *Journal of Agriculture and Food Chemistry*, *68*(50), 14928–14937. https://doi.org/10.1021/acs.jafc.0c06134

Liu, H., Hou, Y., Wang, Y., & Li, Z. (2020b). Enhancement of sulfur conversion rate in the production of L-cysteine by engineered *Escherichia coli*. *Journal of Agriculture and Food Chemistry*, *68*(1), 250–257. https://doi.org/10.1021/acs.jafc.9b06330

Liu, H., Zhang, H., Wang, S., Cui, J., Weng, W., Liu, X., Tang, H., Hu, Y., Li, X., Zhang, K., Zhou, F., Jing, Y., & Su, J. (2023). Bone-targeted bioengineered bacterial extracellular vesicles delivering siRNA to ameliorate osteoporosis. *Composites Part B: Engineering*, *255*, 110610. https://doi.org/10.1016/j.compositesb.2023.110610

Liu, H., Geng, Z., & Su, J. (2022a). Engineered mammalian and bacterial extracellular vesicles as promising nanocarriers for targeted therapy. *Extracellular Vesicles and Circulating Nucleic Acids*, *3*, 63–86. https://doi.org/10.20517/evcna.2022.04

Liu, H., Li, M., Zhang, T., Liu, X., Zhang, H., Geng, Z., & Su, J. (2022b). Engineered bacterial extracellular vesicles for osteoporosis therapy. *Chemical Engineering Journal*, *450*, 138309. https://doi.org/10.1016/j.cej.2022.138309</bib>

Han Liu, H. Z., Han, Y., Hu, Y., Geng, Z., & Su, J. (2022). Bacterial extracellular vesicles-based therapeutic strategies for bone and soft tissue tumors therapy. *Theranostics*, *12*(15), 6576–6594.

Alvarez-Erviti, L., Seow, Y., Yin, H., Betts, C., Lakhal, S., & Wood, M. J. (2011). Delivery of siRNA to the mouse brain by systemic injection of targeted exosomes. *Nature Biotechnology*, *29*(4), 341–345. https://doi.org/10.1038/nbt.1807

Cheng, K., Zhao, R., Li, Y., Qi, Y., Wang, Y., Zhang, Y., Qin, H., Qin, Y., Chen, L., Li, C., Liang, J., Li, Y., Xu, J., Han, X., Anderson, G. J., Shi, J., Ren, L., Zhao, X., & Nie, G. (2021). Bioengineered bacteria-derived outer membrane vesicles as a versatile antigen display platform for tumor vaccination via Plug-and-Display technology. *Nature Communications*, *12*(1), 2041. https://doi.org/10.1038/s41467-021-22308-8

Liang, Y., Duan, L., Lu, J., & Xia, J. (2021). Engineering exosomes for targeted drug delivery. *Theranostics*, *11*(7), 3183–3195. https://doi.org/10.7150/thno.52570

Ren, X., Chen, X., Geng, Z., & Su, J. (2022). Bone-targeted biomaterials: Strategies and applications. *Chemical Engineering Journal*, *446*, 137133. https://doi.org/10.1016/j.cej.2022.137133

Wang, J., Li, X., Wang, S., Cui, J., Ren, X., & Su, J. (2023). Bone-targeted exosomes: Strategies and applications. *Advances Healthcare Materials*, *12*(18), e2203361. https://doi.org/10.1002/adhm.202203361

Zeng, Z. L., & Xie, H. (2022). Mesenchymal stem cell-derived extracellular vesicles: A possible therapeutic strategy for orthopaedic diseases: A narrative review. *Biomaterials Translation*, *3*(3), 175–187. https://doi.org/10.12336/biomatertransl.2022.03.002

Guo, J., Wang, F., Hu, Y., Luo, Y., Wei, Y., Xu, K., Zhang, H., Liu, H., Bo, L., Lv, S., Sheng, S., Zhuang, X., Zhang, T., Xu, C., Chen, X., & Su, J. (2023). Exosome-based bone-targeting drug delivery alleviates impaired osteoblastic bone formation and bone loss in inflammatory bowel diseases. *Cell Reports Medicine*, *4*(1), 100881. https://doi.org/10.1016/j.xcrm.2022.100881

Wu, M., Chen, G., & Li, Y. P. (2016). TGF-β and BMP signaling in osteoblast, skeletal development, and bone formation, homeostasis and disease. *Bone Research*, *4*, 16009. https://doi.org/10.1038/boneres.2016.9

Xu, Y., Yang, Y., Hua, Z., Li, S., Yang, Z., Liu, Q., Fu, G., Ji, P., & Wu, Q. (2021). BMP2 immune complexes promote new bone formation by facilitating the direct contact between osteoclasts and osteoblasts. *Biomaterials*, *275*, 120890. https://doi.org/10.1016/j.biomaterials.2021.120890

Fan, Q., Bai, J., Shan, H., Fei, Z., Chen, H., Xu, J., Ma, Q., Zhou, X., & Wang, C. (2021). Implantable blood clot loaded with BMP-2 for regulation of osteoimmunology and enhancement of bone repair. *Bioactive Materials*, *6*(11), 4014–4026. https://doi.org/10.1016/j.bioactmat.2021.04.008

Gujrati, V., Prakash, J., Malekzadeh-Najafabadi, J., Stiel, A., Klemm, U., Mettenleiter, G., Aichler, M., Walch, A., & Ntziachristos, V. (2019). Bioengineered bacterial vesicles as biological nano-heaters for optoacoustic imaging. *Nature Communications*, *10*(1), 1114. https://doi.org/10.1038/s41467-019-09034-y

Li, Y., Zhao, R., Cheng, K., Zhang, K., Wang, Y., Zhang, Y., Li, Y., Liu, G., Xu, J., Xu, J., Anderson, G. J., Shi, J., Ren, L., Zhao, X., & Nie, G. (2020). Bacterial outer membrane vesicles presenting programmed death 1 for improved cancer immunotherapy via immune activation and checkpoint inhibition. *ACS Nano*, *14*(12), 16698–16711. https://doi.org/10.1021/acsnano.0c03776

Thomas, S. C., Madaan, T., Kamble, N. S., Siddiqui, N. A., Pauletti, G. M., & Kotagiri, N. (2022). Engineered bacteria enhance immunotherapy and targeted therapy through stromal remodeling of tumors. *Advanced Healthcare Materials*, *11*(2), e2101487. https://doi.org/10.1002/adhm.202101487

Guo, M., Liu, H., Yu, Y., Zhu, X., Xie, H., Wei, C., Mei, C., Shi, Y., Zhou, N., Qin, K., & Li, W. (2023). Lactobacillus rhamnosus GG ameliorates osteoporosis in ovariectomized rats by regulating the Th17/Treg balance and gut microbiota structure. *Gut Microbes*, *15*(1), 2190304. https://doi.org/10.1080/19490976.2023.2190304

Rachner, T. D., Khosla, S., & Hofbauer, L. C. (2011). Osteoporosis: Now and the future. *Lancet*, *377*(9773), 1276–1287. https://doi.org/10.1016/s0140-6736(10)62349-5

Bone, H. G., Wagman, R. B., Brandi, M. L., Brown, J. P., Chapurlat, R., Cummings, S. R., Czerwiński, E., Fahrleitner-Pammer, A., Kendler, D. L., Lippuner, K., Reginster, J. Y., Roux, C., Malouf, J., Bradley, M. N., Daizadeh, N. S., Wang, A., Dakin, P., Pannacciulli, N., Dempster, D. W., & Papapoulos, S. (2017). 10 years of denosumab treatment in postmenopausal women with osteoporosis: results from the phase 3 randomised FREEDOM trial and open-label extension. *Lancet Diabetes Endocrinology*, *5*(7), 513–523. https://doi.org/10.1016/s2213-8587(17)30138-9

Neer, R. M., Arnaud, C. D., Zanchetta, J. R., Prince, R., Gaich, G. A., Reginster, J. Y., Hodsman, A. B., Eriksen, E. F., Ish-Shalom, S., Genant, H. K., Wang, O., & Mitlak, B. H. (2001). Effect of parathyroid hormone (1-34) on fractures and bone mineral density in postmenopausal women with osteoporosis. *New England Journal of Medicine*, *344*(19), 1434–1441. https://doi.org/10.1056/nejm200105103441904

Zhou, Y., Deng, Y., Liu, Z., Yin, M., Hou, M., Zhao, Z., Zhou, X., & Yin, L. (2021). Cytokine-scavenging nanodecoys reconstruct osteoclast/osteoblast balance toward the treatment of postmenopausal osteoporosis. *Science Advances*, *7*(48), eabl6432. https://doi.org/10.1126/sciadv.abl6432

Lyu, Z., Hu, Y., Guo, Y., & Liu, D. (2023). Modulation of bone remodeling by the gut microbiota: A new therapy for osteoporosis. *Bone Research*, *11*(1), 31. https://doi.org/10.1038/s41413-023-00264-x

Zaiss, M. M., Jones, R. M., Schett, G., & Pacifici, R. (2019). The gut-bone axis: How bacterial metabolites bridge the distance. *Journal of Clinical Investment*, *129*(8), 3018–3028. https://doi.org/10.1172/jci128521

Liu, H., Li, M., Zhang, T., Liu, X., Zhang, H., Geng, Z., & Su, J. (2022c). Engineered bacterial extracellular vesicles for osteoporosis therapy. *Chemical Engineering Journal*, *450*, 138309. https://doi.org/10.1016/j.cej.2022.138309

Chen, C. Y., Rao, S. S., Yue, T., Tan, Y. J., Yin, H., Chen, L. J., Luo, M. J., Wang, Z., Wang, Y. Y., Hong, C. G., Qian, Y. X., He, Z. H., Liu, J. H., Yang, F., Huang, F. Y., Tang, S. Y., & Xie, H. (2022). Glucocorticoid-induced loss of beneficial gut bacterial extracellular vesicles is associated with the pathogenesis of osteonecrosis. *Science Advances*, *8*(15), eabg8335. https://doi.org/10.1126/sciadv.abg8335

Liu, H., Zhang, H., Han, Y., Hu, Y., Geng, Z., & Su, J. (2022d). Bacterial extracellular vesicles-based therapeutic strategies for bone and soft tissue tumors therapy. *Theranostics*, *12*(15), 6576–6594. https://doi.org/10.7150/thno.78034

Cheng, L., & Hill, A. F. (2022). Therapeutically harnessing extracellular vesicles. *Nature Reviews Drug Discovery*, *21*, 379–399. https://doi.org/10.1038/s41573-022-00410-w

Cong, M., Tan, S., Li, S., Gao, L., Huang, L., Zhang, H. G., & Qiao, H. (2022). Technology insight: Plant-derived vesicles-How far from the clinical biotherapeutics and therapeutic drug carriers? *Advanced Drug Delivery Reviews*, *182*, 114108. https://doi.org/10.1016/j.addr.2021.114108

Liu, H., Sun, J., Wang, M., Wang, S., Su, J., & Xu, C. (2023). Intestinal organoids and organoids extracellular vesicles for inflammatory bowel disease treatment. *Chemical Engineering Journal*, *465*, 142842. https://doi.org/10.1016/j.cej.2023.142842

Liu, H., & Su, J. (2023). Organoid and organoid extracellular vesicles for osteoporotic fractures therapy: Current status and future perspectives. *Interdisciplinary Medicine*, *1*(3), e20230011.

Wu, P., Zhang, B., Ocansey, D. K. W., Xu, W., & Qian, H. (2021). Extracellular vesicles: A bright star of nanomedicine. *Biomaterials*, *269*, 120467. https://doi.org/10.1016/j.biomaterials.2020.120467

Chen, Q., Bai, H., Wu, W., Huang, G., Li, Y., Wu, M., Tang, G., & Ping, Y. (2020). Bioengineering bacterial vesicle-coated polymeric nanomedicine for enhanced cancer immunotherapy and metastasis prevention. *Nano Letters*, *20*(1), 11–21. https://doi.org/10.1021/acs.nanolett.9b02182

Yue, Y., Xu, J., Li, Y., Cheng, K., Feng, Q., Ma, X., Ma, N., Zhang, T., Wang, X., Zhao, X., & Nie, G. (2022). Antigen-bearing outer membrane vesicles as tumour vaccines produced in situ by ingested genetically engineered bacteria. *Nature Biomedical Engineering*, *6*(7), 898–909. https://doi.org/10.1038/s41551-022-00886-2

Fu, H., Wang, L., Bao, Q., Ni, D., Hu, P., & Shi, J. (2022). Acid neutralization and immune regulation by calcium–aluminum-layered double hydroxide for osteoporosis reversion. *Journal of the American Chemical Society*, *144*(20), 8987–8999.

SUPPORTING INFORMATION

Additional supporting information can be found online in the Supporting Information section at the end of this article.

How to cite this article: Liu, H., Song, P., Zhang, H., Zhou, F., Ji, N., Wang, M., Zhou, G., Han, R., Liu, X., Weng, W., Tan, H., Wang, S., Zheng, L., Jing, Y., & Su, J. (2024). Synthetic biology-based bacterial extracellular vesicles displaying BMP-2 and CXCR4 to ameliorate osteoporosis. *Journal of Extracellular Vesicles*, *13*, e12429. https://doi.org/10.1002/jev2.12429